

Shortcuts in Domain Walls and the Horizon Problem

Elcio Abdalla and Bertha Cuadros-Melgar

Instituto de Fisica, Universidade de São Paulo
C.P.66.318, CEP 05315-970, São Paulo, Brazil.

Abstract

We consider a dynamical membrane world in a space-time with scalar bulk matter described by domain walls. Using the solutions to Einstein field equations and Israel conditions we investigate the possibility of having shortcuts for gravitons leaving the wall and returning subsequently. As it turns out, they usually appear under mild conditions.

In the comparison with photons following a geodesic inside the brane, we verify that shortcuts exist. For some Universes they are small, but there are cases where shortcuts are effective enough to imply a solution of the horizon problem. In such cases shortcuts can be physically valuable.

1 Introduction

Although standard model of particle physics has been established as the uncontested theory of all interactions down to distances of 10^{-17} m, there are good reasons to believe that there is a new physics arising soon at the experimental level [1]. On the other hand, string theory provides an excellent background to solve long standing problems of theoretical high energy physics. It is by now a widespread idea that M-theory [2] is a reasonable description of our Universe. In the field theory limit, it is described by a solution of the (eventually 11-dimensional) Einstein equations with a cosmological constant by means of a four dimensional membrane. In this picture only gravity survives in the extra dimensions, while the remaining matter and gauge interactions are typically four dimensional.

In this picture, there is a possibility that gravitational fields, while propagating out of the brane speed up, reaching farther distances in smaller time as compared to light propagating inside the brane, a scenario that for a resident of the brane (as ourselves) implies shortcuts [3]—[7].

This possibility implies that we can have alternatives to the inflationary scenario in order to explain the homogeneity problem in cosmology. Recently, this scenario has been proposed as an actually realizable possibility [9, 10]. In [9] it has been shown that in some scenarios shortcuts are very difficult to be detected today because of the extremely short delay of the photon as compared to the graviton coming from the same source, but before nucleosynthesis delays are large enough to imply thermalization of the whole universe, thus providing a possible solution to the homogeneity problem [9], alternative [10] to inflation [12]. In the case of domain walls shortcuts are also common.

Recently it has been proved [13] that brane Universes can provide a means for finding relics of the higher dimensions in the cosmic microwave background as well. Thus it is worthwhile further pursuing brane models as useful tools to understand the physics of strings and M-theory [14], which proves them as very important instances to try a better insight of the Universe and its properties.

2 The General Setup

We consider a scenario described by the gravitational action in a D-dimensional bulk with a scalar field, a bulk dilaton, a domain wall potential and a Gibbons-Hawking term [15],

$$S = \int_{bulk} d^D x \sqrt{-g} \left(\frac{1}{2} R - \frac{1}{2} (\partial\phi)^2 - V(\phi) \right) - \int_{dw} d^{D-1} x \sqrt{-h} ([K] + \hat{V}(\phi)), \quad (1)$$

where ϕ is the bulk dilaton, K is the extrinsic curvature, $V(\phi)$ and $\hat{V}(\phi)$ are bulk and domain wall potentials, respectively. These are here considered to be of the Liouville type:

$$V(\phi) = V_0 e^{\beta\phi}, \quad (2)$$

$$\hat{V}(\phi) = \hat{V}_0 e^{\alpha\phi}. \quad (3)$$

We consider the bulk metric as being static and invariant under rotation, being given by

$$ds^2 = -U(r)dt^2 + U(r)^{-1}dr^2 + R(r)^2d\Omega_k^2, \quad (4)$$

where $d\Omega_k^2$ is the line element on a $D - 2$ dimensional space of constant curvature depending on a parameter k . Such a metric is supposed to have a mirror symmetry Z_2 with respect to the domain wall. Such a symmetry will be used in order to impose the Israel conditions [16]. In fact, the variation of the total action (1) including the Gibbons-Hawking term leads directly to the Israel conditions which in view of the Z_2 symmetry become

$$K_{MN} = -\frac{1}{2(D-2)}\hat{V}(\phi)h_{MN} \quad . \quad (5)$$

The extrinsic curvature can be computed as

$$K_{MN} = h_M^P h_N^Q \nabla_P n_Q \quad , \quad (6)$$

where the unit normal, which points into $r < r(t)$, is

$$n_M = \frac{1}{\sqrt{U - \dot{r}^2}}(\dot{r}, -1, 0 \dots, 0). \quad (7)$$

The ij component of (5) can be written as

$$\frac{R'}{R} = \frac{\hat{V}(\phi)}{2(D-2)U}\sqrt{U - \frac{\dot{r}^2}{U}}, \quad (8)$$

while the 00 component is

$$\left(\frac{R'}{R}\right)^{-1} \left(\frac{R'}{R}\right)' = \frac{\hat{V}'(\phi)}{\hat{V}(\phi)} - \frac{R'}{R}. \quad (9)$$

The equation of motion for the dilaton obtained from the action (1), together with (9), can be simultaneously solved with the Ansatz (4), leading to [17]

$$\phi(r) = \phi_\star - \frac{\alpha(D-2)}{\alpha^2(D-2)+1}\log r, \quad (10)$$

$$R(r) = (\alpha^2(D-2)+1)C\hat{V}_0 e^{\alpha\phi_\star} r^{\frac{1}{\alpha^2(D-2)+1}}, \quad (11)$$

where ϕ_\star and C are arbitrary integration constants.

The motion of the domain wall is governed by the ij component of the Israel conditions (8). That equation can be written in terms of the brane proper time τ as

$$\frac{1}{2} \left(\frac{dR}{d\tau} \right)^2 + F(R) = 0. \quad (12)$$

The induced metric on the domain wall is Friedmann-Robertson-Walker and (12) describes the evolution of the scale factor $R(\tau)$. This equation is the same as that one for a particle of unit mass and zero energy rolling in a potential $F(R)$ given by

$$F(R) = \frac{1}{2} U R'^2 - \frac{1}{8(D-2)^2} \hat{V}^2 R^2. \quad (13)$$

Notice that the solution only exists when $F(R) \leq 0$.

From the induced domain wall metric we find the relations between the time parameter in the brane (τ) and in the bulk (t) as given by

$$dt = \frac{\sqrt{U + \left(\frac{dr}{d\tau} \right)^2}}{U} d\tau,$$

so that

$$\frac{dr}{dt} = \frac{dr}{d\tau} \frac{d\tau}{dt} = \frac{dr}{d\tau} \frac{U}{\sqrt{U + \left(\frac{dr}{d\tau} \right)^2}}, \quad (14)$$

where $\frac{dr}{d\tau} = \frac{dR}{d\tau} \left(\frac{dR}{dr} \right)^{-1}$ can be obtained from (12).

Consider two points on the brane. In general, there are more than one null geodesic connecting them in the D-dimensional spacetime. The trajectories of photons must be on the brane and those of gravitons may be outside. We consider the shortest path for both photons and gravitons. For the latter, the geodesic equation is the same as the one considered in [3], since the bulk metric is static:

$$\ddot{r}_g + \left(\frac{1}{r_g} - \frac{3}{2} \frac{U'}{U} \right) \dot{r}_g^2 + \frac{1}{2} U U' - \frac{U^2}{r_g} = 0. \quad (15)$$

The solutions of (14) and (15) in terms of the bulk proper time t were obtained by means of a **MAPLE** program. Now we discuss the possibility of shortcuts in the cases of the various solutions describing different Universes defined by the domain wall solution.

3 Solutions of the Geodesic Equation

3.1 Type I Solutions

We define the type I brane solutions as those for which $\alpha = \beta = 0$. Consequently, the potentials become cosmological constants. The solution also has a constant dilaton $\phi = \phi_0$. A simple rescaling in the metric leads us to

$$ds^2 = -U(R)dt^2 + U(R)^{-1}dR^2 + R^2d\Omega_k^2, \quad (16)$$

with

$$U(R) = k - 2MR^{-(D-3)} - \frac{2V_0}{(D-1)(D-2)}R^2, \quad (17)$$

which corresponds to a topological black hole solution in D dimensions with a cosmological constant.

As discussed in Ref. [17], if the domain wall has positive energy density ($\hat{V}_0 > 0$), the relevant part of the bulk spacetime is $R < R(\tau)$, which is the region containing the singularity. If it has negative energy density ($\hat{V}_0 < 0$), the relevant part is $R > R(\tau)$, which is non-singular unless the wall reaches $R = 0$.

The potential $F(R)$ ruling the evolution of the scale factor is

$$F(R) = \frac{k}{2} - MR^{-(D-3)} - \hat{\Lambda}R^2, \quad (18)$$

where the effective cosmological constant on the domain wall is given by

$$\hat{\Lambda} = \frac{1}{D-2} \left[\frac{V_0}{D-1} + \frac{\hat{V}_0^2}{8(D-2)} \right]. \quad (19)$$

We shall analyze each of the four cases presented in [17]. As we have previously stated, the equation of motion (12) has a solution only when $F(R) \leq 0$. This is automatic only if $U(R) < 0$, i.e. if r is a time coordinate; therefore, we look for solutions with $U(R) > 0$. In fact, both conditions,

$$F(R) \leq 0 \quad \text{and} \quad U(R) > 0, \quad (20)$$

can coexist in some cases as we will see in what follows.

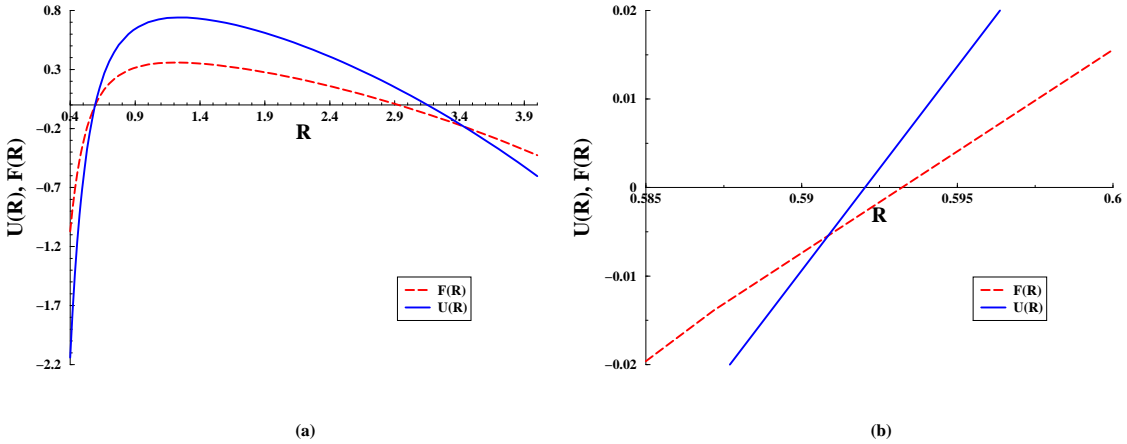


Figure 1: (a) $U(R)$ and $F(R)$ for type I solutions with $M = 1/10$, $V_0 = 1$ and $\hat{V}_0 = \pm 1$, (b) Zoom of the event horizon region.

3.1.1 $\hat{\Lambda} > 0$, $M > 0$

From the graph of $U(R)$ (see Fig.1) we can choose the initial condition for the domain wall assuming that (17) describes a dS-Schwarzschild bulk with event and cosmological horizons when $M > 0$ and $V_0 > 0$.

We thus choose the initial condition for the domain wall inside this region and where r is a space coordinate. From Fig.1 let us notice that there are two small regions, $r_H \leq r < 0.593$ and $2.93 \leq r < r_C$, where (20) holds. The results are shown in Fig.2. We see that for region I the geodesics follow the domain wall for a while and then decouple falling into the event horizon. For region II all the geodesics and the domain wall converge to the cosmological horizon r_C independently of the value of \hat{V}_0 .

3.1.2 $\hat{\Lambda} < 0$, $M > 0$

This case describes an AdS-Schwarzschild bulk. The condition (20) is full-filled inside a very small range as we can see in Fig.3(a). However, all the geodesics fall into the event horizon after following some path on the brane

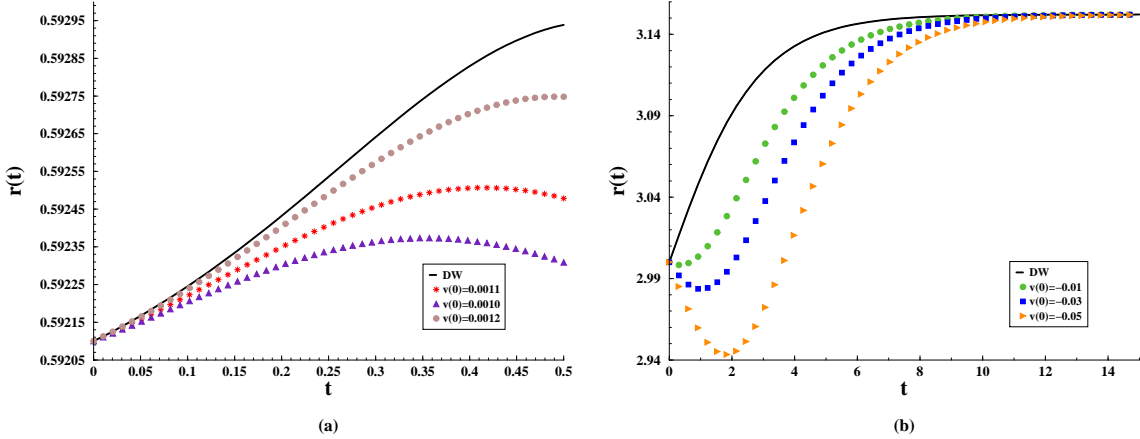


Figure 2: Domain wall motion and geodesics for type I solutions with $M = 1/10$, $V_0 = 1$ and $\hat{V}_0 = 1$ in (a) region I and, (b) region II.

(see Fig.3(b)).

3.1.3 $\hat{\Lambda} > 0, M < 0$

From Fig.4(a) we choose the initial condition for the domain wall equation of motion inside the region where (20) holds. As we can see from Fig.4(b), the domain wall and the geodesic converge to the cosmological horizon r_C . However, after some threshold initial velocity the geodesics diverge to the timelike naked singularity.

3.1.4 $\hat{\Lambda} < 0, M < 0$

In this case (12) can only have solution when $k = -1$. This is a topological black hole in an asymptotically AdS space. From Fig.5 we see that there is no solution fulfilling (20) between event and cosmological horizons.

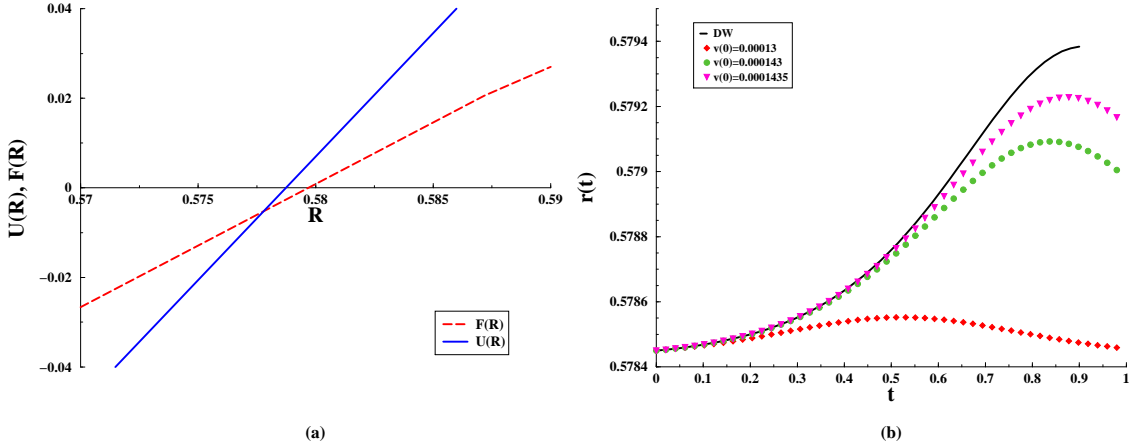


Figure 3: (a) Zoom of the region where (20) holds from the graph of $U(R)$ and $F(R)$ with $\hat{\Lambda} < 0$ and $M > 0$ for type I solutions, (b) Domain wall motion and geodesics for type I solutions with $M = 1/10$, $V_0 = -1$ and $\hat{V}_0 = 1$.

3.2 Type II Solutions

The type II solutions have $\alpha = \beta/2$ and $k = 0$. The metric is given by

$$U(r) = (1 + b^2)^2 r^{\frac{2}{1+b^2}} \left(-2Mr^{-\frac{D-1-b^2}{1+b^2}} - \frac{2\Lambda}{(D-1-b^2)} \right), \quad (21)$$

and the scale factor is

$$R(r) = r^{\frac{1}{1+b^2}}, \quad (22)$$

where

$$\Lambda = \frac{V_0 e^{2b\phi_0}}{D-2}, \quad (23)$$

$$b = \frac{1}{2}\beta\sqrt{D-2}. \quad (24)$$

The potential is given by the expression

$$F(R) = -R^{2(1-b^2)} \left(MR^{-(D-1-b^2)} + \hat{\Lambda} \right), \quad (25)$$

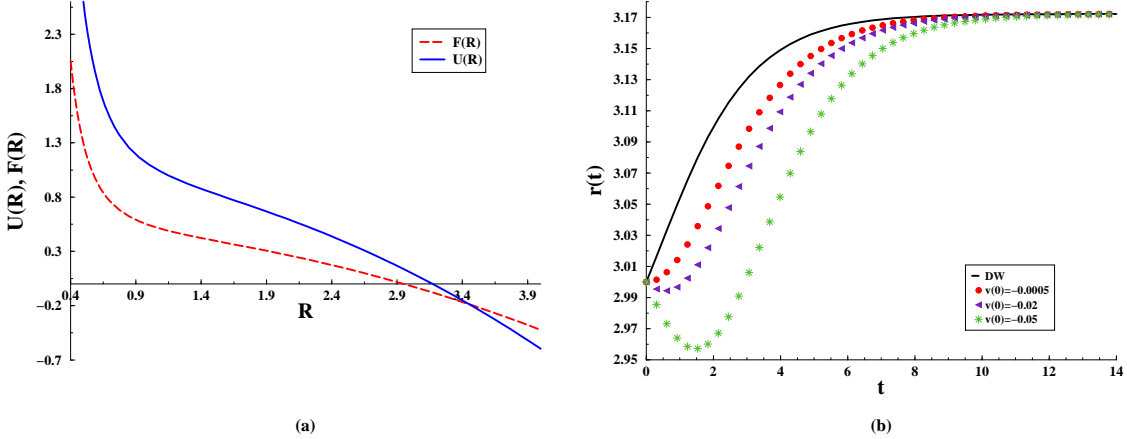


Figure 4: (a) $U(R)$ and $F(R)$ with $\hat{\Lambda} > 0$ and $M < 0$ for type I solutions, (b) Domain wall motion and geodesics for $M = -1/10$, $V_0 = 1$ and $\hat{V}_0 = 1$.

where

$$\hat{\Lambda} = \frac{e^{2b\phi_0}}{D-2} \left(\frac{V_0}{D-1-b^2} + \frac{\hat{V}_0^2}{8(D-2)} \right). \quad (26)$$

There are twelve cases from which we choose those ones where r is a spatial coordinate. When $b^2 < D-1$, r is a spatial coordinate if $V_0 < 0$. When $b^2 > D-1$, r is spatial if $M < 0$.

We should also rewrite (20) as

$$F(r) \leq 0 \quad \text{and} \quad U(r) > 0. \quad (27)$$

3.2.1 $\hat{\Lambda} > 0$, $M < 0$, $b^2 > D-1$

In this case $U(r)$ is always positive, whereas $F(r)$ is negative for small r . From Fig.6 we see that some microscopic shortcuts appear in the very beginning of the solution and after crossing the domain wall they escape to infinity.

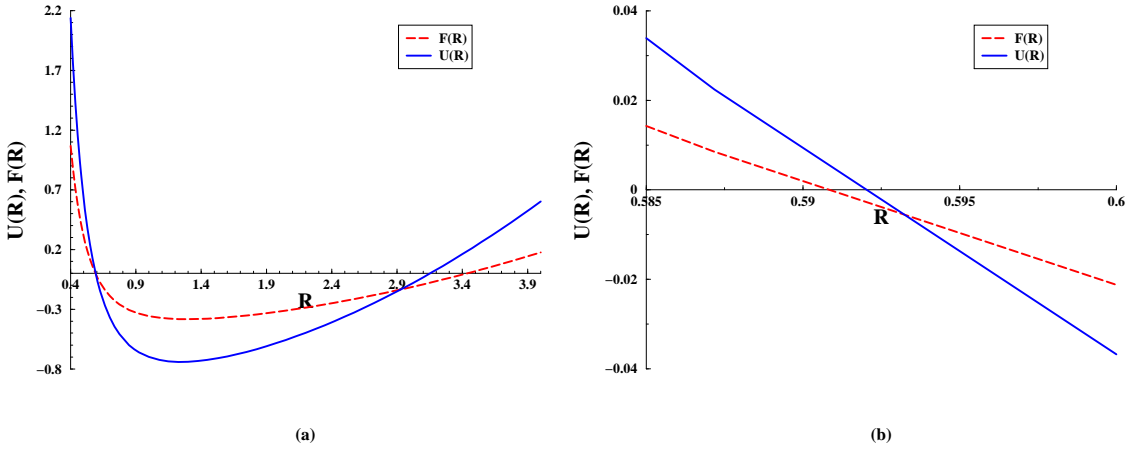


Figure 5: (a) $U(R)$ and $F(R)$ with $\hat{\Lambda} < 0$ and $M = -1/10$ for type I solutions, (b) Zoom of the event horizon region.

3.2.2 $\hat{\Lambda} < 0, M > 0, b^2 < 1$

This case describes a black $(D - 2)$ brane solution in AdS space. Here there is a very small region where (27) holds after the event horizon as we can see from Fig.7. We show the entire domain wall solution and we see that geodesics follow it and then decouple to fall into the event horizon at later times.

3.2.3 $\hat{\Lambda} < 0, M > 0, 1 < b^2 < D - 1$

This case is also a black brane in AdS space. The region where (27) is respected is shown in Fig.8. As in the previous case all the geodesics follow the domain wall and at later times fall into the event horizon.

3.2.4 $\hat{\Lambda} < 0, M < 0$

As $F(r)$ is always positive for all b^2 , no solutions to (14) exist.

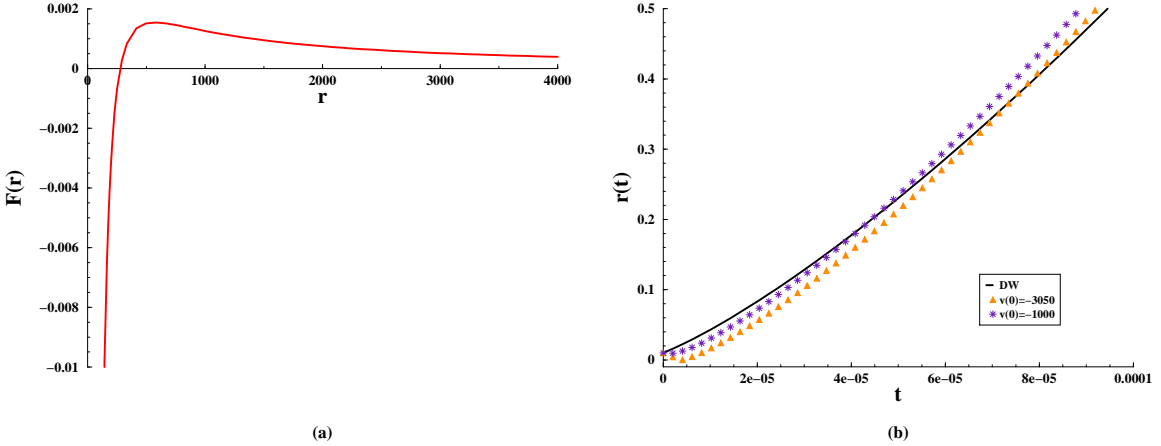


Figure 6: (a) $F(r)$ with $\hat{\Lambda} > 0$ and $M < 0$ for type II solutions, (b) Domain wall motion and geodesics for $V_0 = 1$, $\hat{V}_0 = 6$, $M = -10$ and $\beta = \sqrt{10}$.

3.3 Type III Solutions

The type III solutions have $\alpha = \frac{2}{\beta(D-2)}$. In this case, the metric is given by

$$U(r) = (1 + b^2)^2 r^{\frac{2}{1+b^2}} \left(-2Mr^{\frac{-1+b^2(D-3)}{1+b^2}} - \frac{2\Lambda}{(1 + b^2(D-3))} \right), \quad (28)$$

and the scale factor is

$$R(r) = \gamma r^{\frac{b^2}{1+b^2}}, \quad (29)$$

where

$$\gamma = \left(\frac{(D-3)}{2k\Lambda(1-b^2)} \right)^{\frac{1}{2}}. \quad (30)$$

The values of Λ and b are the same as those given in (23) and (24).

The potential $F(R)$ is

$$F(R) = -\frac{(D-3)b^4}{2k(1-b^2)(1+b^2(D-3))} - M\gamma^2 b^4 \left(\frac{R}{\gamma} \right)^{-(D-3+\frac{1}{b^2})} -$$

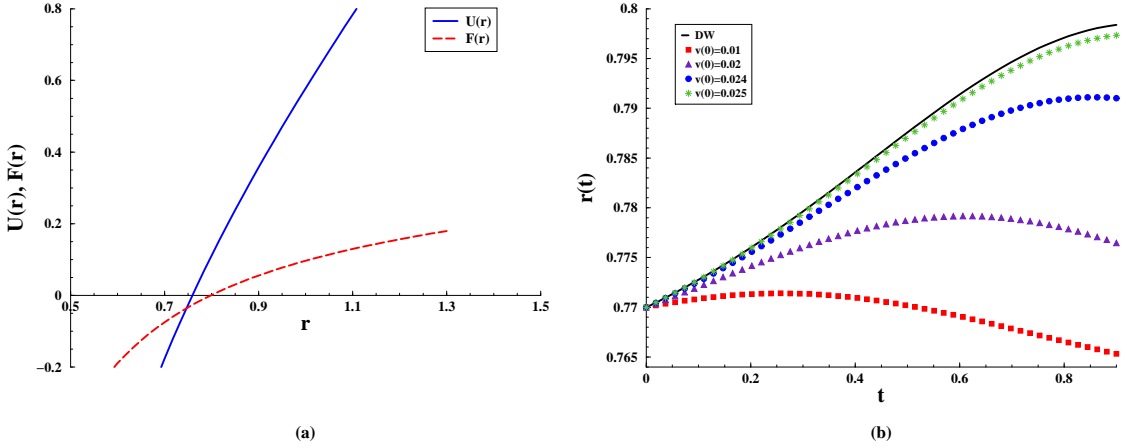


Figure 7: (a) $U(r)$ and $F(r)$ with $\hat{\Lambda} < 0$ and $M > 0$ for type II solutions, (b) Domain wall motion and geodesics for $V_0 = -1$, $\hat{V}_0 = 1$, $M = 1/10$ and $\beta = 1/\sqrt{2}$.

$$-\frac{\hat{V}_0^2 e^{\frac{2\phi_0}{b}} \gamma^2}{8(D-2)^2} \left(\frac{R}{\gamma}\right)^{-2\left(\frac{1}{b^2}-1\right)}. \quad (31)$$

If $V_0 > 0$, r turns out to be a time coordinate, while for $V_0 < 0$, it is a spatial coordinate. From the twelve cases shown in [17] we choose those where it is a spatial coordinate. For all these solutions the condition (27) applies.

3.3.1 $V_0 < 0$, $M > 0$, $b^2 < \frac{1}{(D-1)}$

This case describes a topological black hole in AdS space. From Fig.9 we can see the region where (27) holds. There are no shortcuts in this interval, and all the geodesics follow the brane and then either diverge to infinity or fall into the event horizon.

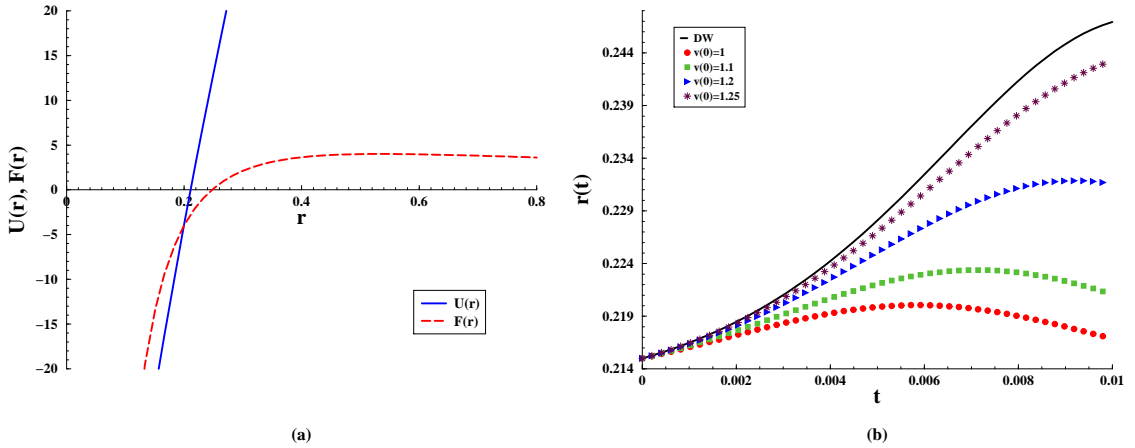


Figure 8: (a) $U(r)$ and $F(r)$ with $\hat{\Lambda} < 0$ and $M > 0$ for type II solutions, (b) Domain wall motion and geodesics for $V_0 = -1$, $\hat{V}_0 = 1$, $M = 10$ and $\beta = 2$.

3.3.2 $V_0 < 0$, $M > 0$, $\frac{1}{(D-1)} < b^2 < 1$

We again have a topological black hole in AdS space. There is a small interval where (14) has solution as we can see from Fig.10(a). Our results are shown in Fig.10(b). Notice that the domain wall equation of motion has a solution only inside the interval shown there. This means that only a group of geodesics with initial velocity $\dot{r}(0) > v_c$ can meet the domain wall after a roundabout in the bulk. It is also shown that negative initial velocities force geodesics to fall into the event horizon.

3.3.3 $V_0 < 0$, $M > 0$, $b^2 > 1$

The black hole in AdS space appearing here has round spatial section. In this case $U(r)$ is always positive (then r is always a spatial coordinate); however, as we must fulfill (27), we should notice that $F(r) \leq 0$ for $r \geq 3 * 10^5$. We found that shortcuts are possible for several initial velocities if $M = 0$.

The case $M > 0$ is shown in Fig.11. We have two regions of interest after the event horizon depending only on the sign of $F(r)$ since $U(r)$ is positive

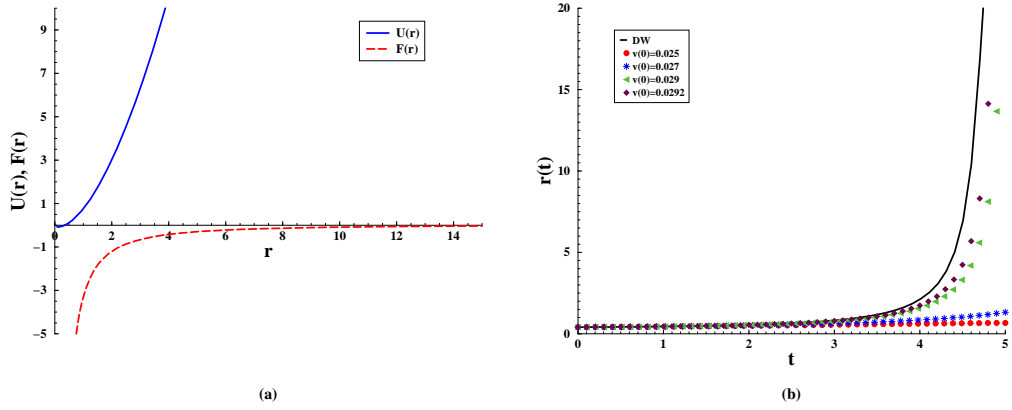


Figure 9: (a) $U(r)$ and $F(r)$ for Type III solutions with $k = -1$, $M = 1/10$ and $\beta^2 < \frac{1}{(D-2)}$, (b) Domain Wall motion and geodesics for $V_0 = -1$, $\hat{V}_0 = 1$, $\phi_0 = 1$ and $\beta = 1/\sqrt{6}$.

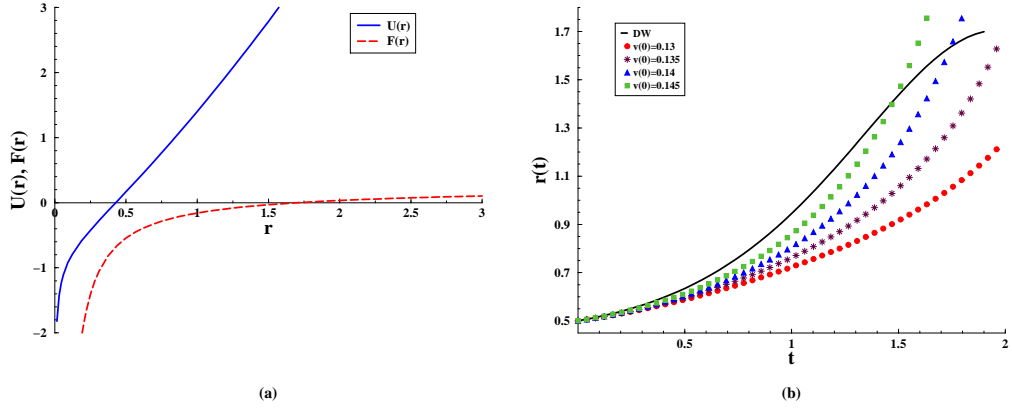


Figure 10: (a) $U(r)$ and $F(r)$ for $k = -1$, $M = 1/10$ and $V_0 < 0$ in Type III solutions, (b) Domain wall motion and geodesics with $V_0 = -1$, $\hat{V}_0 = 1$, $\phi_0 = 1$ and $\beta = 1/\sqrt{2}$.

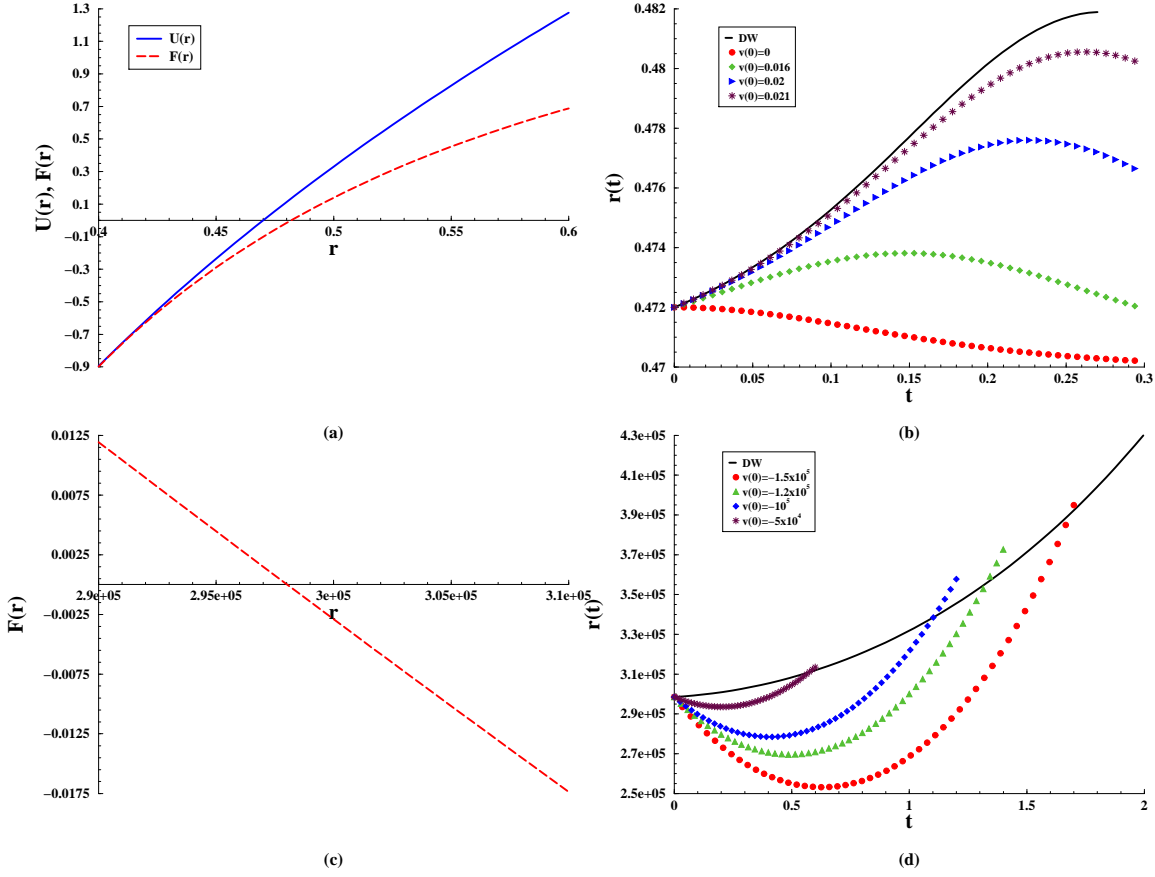


Figure 11: (a) $U(r)$ and $F(r)$ for $M = 1/10$ and $V_0 < 0$ in Type III solutions, (b) Domain wall motion and geodesics with $V_0 = -1$, $\hat{V}_0 = 1$, $\phi_0 = 1$ and $\beta = \sqrt{5}/2$, (c) $F(r)$ in the region of interest, (d) Domain wall motion and geodesics under the same conditions as (b).

in this range. In the first region all the geodesics initially follow the brane and fall into the event horizon at later times. In the second region we have shortcuts again for several initial velocities.

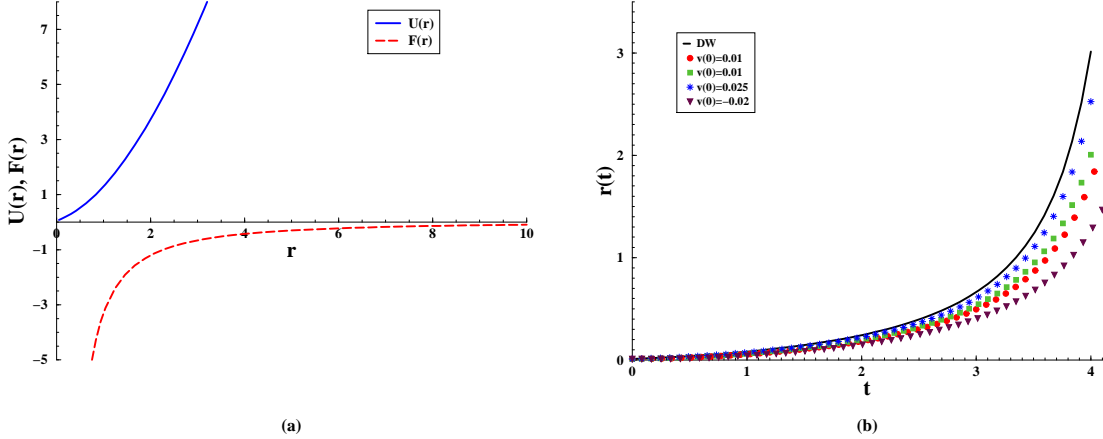


Figure 12: (a) $U(r)$ and $F(r)$ for type III solutions when $k = -1$, $M = -1/10$ and $b^2 < \frac{1}{(D-2)}$, (b) Domain wall motion and geodesics for $V_0 = -1$, $\hat{V}_0 = 1$, $\phi_0 = 1$ and $\beta = 1/\sqrt{6}$.

3.3.4 $V_0 < 0$, $M < 0$, $b^2 < \frac{1}{(D-1)}$

Here $U(r)$ is always positive while $F(r)$ is negative in the range shown in Fig.12. The domain wall and the geodesics diverge after some time near the end of the range where (14) has a solution.

3.3.5 $V_0 < 0$, $M < 0$, $\frac{1}{(D-1)} < b^2 < 1$

In this case $U(r)$ is always positive while $F(r)$ is negative for a small range as seen in Fig.13. There are several shortcuts in the region where the domain wall equation of motion has solution; nevertheless, there is a threshold velocity after which the geodesics can not return. As we can notice from Fig.13(b), the last curve displayed here ($v(0) = -1.04$) can not be considered a real shortcut since it is not a continuous solution of the geodesic equation, but represents a transition between shortcuts and geodesics falling into the naked singularity.

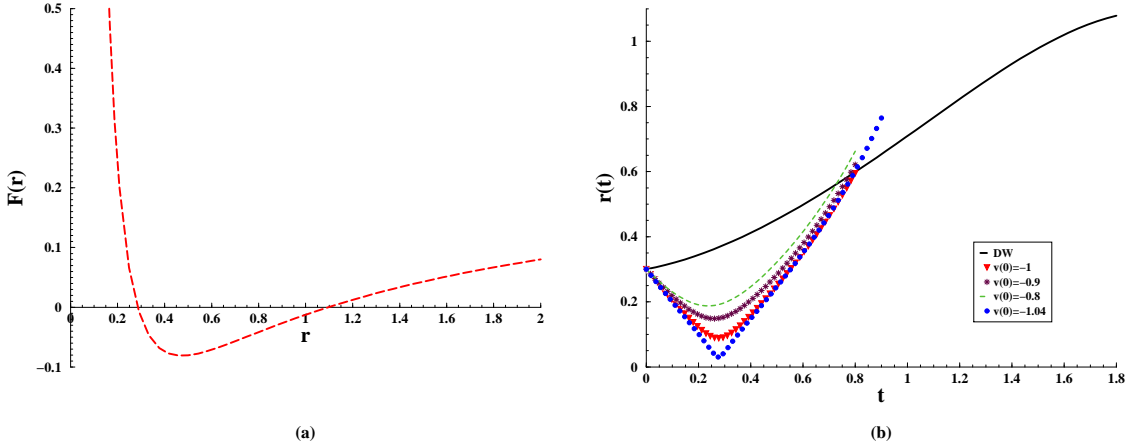


Figure 13: (a) $F(r)$ for type III solutions when $k = -1$, $M = -1/10$ and $\frac{1}{(D-2)} < b^2 < 1$, (b) Domain wall motion and geodesics for $V_0 = -1$, $\hat{V}_0 = 1$, $\phi_0 = 1$ and $\beta = 1/\sqrt{2}$.

3.3.6 $V_0 < 0$, $M < 0$, $b^2 > 1$

Now $U(r)$ is always positive and $F(r)$ will determine the initial condition for the domain wall equation of motion. As we can see from Fig.14, several shortcuts appear.

4 Domain Wall Time and Time Delays

The time delay between the photon traveling on the domain wall and the gravitons traveling in the bulk [9] can be calculated as follows. Since the signals cover the same distance,

$$\int \frac{d\tau_\gamma}{r(\tau_\gamma)} = \int \frac{dt_g}{r_g(t_g)} \sqrt{U(r_g) - \frac{\dot{r}_g(t)^2}{U(r_g)}}, \quad (32)$$

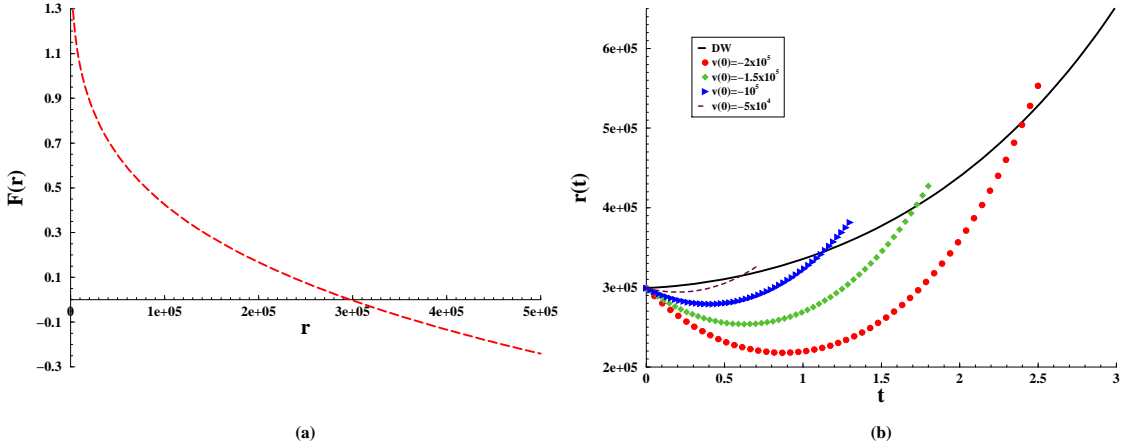


Figure 14: (a) $F(r)$ for type III solutions when $M = -1/10$ and $b^2 > 1$, (b) Domain wall motion and geodesics for $V_0 = -1$, $\hat{V}_0 = 1$, $\phi_0 = 1$ and $\beta = \sqrt{5}/2$.

the difference between photon and graviton time of flight can approximately be written as

$$\frac{\Delta\tau}{r} \simeq \int_0^{\tau_f + \Delta\tau} \frac{d\tau_\gamma}{r(\tau_\gamma)} - \int_0^{\tau_f} \frac{d\tau_g}{r(\tau_g)}, \quad (33)$$

or in terms of the bulk time

$$\Delta\tau \simeq r(t_f) \int_0^{t_f} dt \left(\frac{1}{r_g(t)} \sqrt{U(r_g) - \frac{\dot{r}_g(t)^2}{U(r_g)}} - \frac{1}{r(t)} \frac{d\tau}{dt} \right). \quad (34)$$

The elapsed bulk time t , the corresponding domain wall time τ and the delays (34) are shown in Table 1 for all the shortcut examples considered in the present paper. Notice that $\Delta\tau < 0$ for the last geodesic solution in Fig.13 what, in fact, shows that this curve can not be considered a shortcut (it is probably falling into the naked singularity).

Type II Shortcuts			
Conditions	t	τ	$\Delta\tau$
Fig.6, $v(0) = -3050$	7.5×10^{-5}	0.0025	0.0466
Fig.6, $v(0) = -1000$	4.4×10^{-5}	0.0014	0.0027
Type III Shortcuts			
Fig.10, $v(0) = 0.145$	1.49	0.970	0.210
Fig.10, $v(0) = 0.140$	1.75	1.394	0.523
Fig.11, $v(0) = -5 \times 10^4$	0.58	353	3.51
Fig.11, $v(0) = -10^5$	1.11	683	26.6
Fig.11, $v(0) = -1.2 \times 10^5$	1.33	823	48.1
Fig.11, $v(0) = -1.5 \times 10^5$	1.69	1058	104
Fig.13, $v(0) = -0.8$	0.73	0.753	0.123
Fig.13, $v(0) = -0.9$	0.78	0.808	0.148
Fig.13, $v(0) = -1$	0.81	0.842	0.111
Fig.13, $v(0) = -1.04$	0.80	0.831	-0.129
Fig.14, $v(0) = -5 \times 10^4$	0.61	372	4.11
Fig.14, $v(0) = -10^5$	1.14	703	29.2
Fig.14, $v(0) = -1.5 \times 10^5$	1.72	1081	112
Fig.14, $v(0) = -2 \times 10^5$	2.42	1568	354

Table 1: Domain wall time τ and time delays $\Delta\tau$ for shorcuts appearing in Type II and Type III Solutions

5 Conclusions

We have considered here again the question of shortcuts in a Universe described by a membrane embeded in a bulk with two extra dimensions, the so called dowainwall, described by Einstein gravity with a scalar field. In [17] the full set of solutions of the brane equation of motion and Israel conditions at the wall has been obtained. We studied the possibility of shortcuts in those cases. In one of our previous works we found [3] that in a static brane embeded in a pure Ads space with a black hole (AdS-Schwarzschild, AdS-RN) shortcuts may appear if a certain range of parameters in chosen [9]. Later,

we proved that in a dynamical brane universe shortcuts are actually quite common and may provide an alternative explanation to the horizon problem, since shortcuts are common and very effective before nucleosynthesis, while ineffective, and thus leaving very little trace, today.

Here we further pursue this question and show that under mild conditions shortcuts are common and effective in the sense that the delay can be comparable with the time of travel of the graviton itself. This lends further support to the idea of explaining the horizon problem by means of a thermalization via shortcuts. Although the present model is quite elementary - thus not very realistic - it shows that the mechanism works well.

The question to be answered now is whether more realistic models including e.g. further extra dimensions, such as in the Horava - Witten formulation, can display similar features.

Acknowledgements: This work has been supported by Fundação de Amparo à Pesquisa do Estado de São Paulo (**FAPESP**) and Conselho Nacional de Desenvolvimento Científico e Tecnológico (**CNPq**), Brazil.

References

- [1] M. Gasperini, G. Veneziano, The pre big-bang scenario in String Cosmology, hep-th/0207130.
- [2] J. Polchinski *Superstring Theory* vols. 1 and 2, Cambridge University Press 1998.
- [3] E. Abdalla, A. Casali, B. Cuadros-Melgar, *Nucl. Phys.* **B** to appear, hep-th/0205203.
- [4] C. Csáki, J. Erlich, C. Grojean, *Nucl. Phys.* **B604** 312 (2001), hep-th/0012143.
- [5] H. Ishihara, *Phys. Rev. Lett.* **86**, 381 (2001).
- [6] R. Caldwell and D. Langlois *Phys. Lett.* **B511** (2001) 129-135, gr-qc/0103070.
- [7] D. J. Chung and K. Freese *Phys. Rev.* **D62** (2000) 063513, hep-ph/9910235; *Phys. Rev.* **D61** (2000) 023511, hep-ph/9906542.

- [8] E. Abdalla, B. Cuadros-Melgar, S. Feng, B. Wang *Phys. Rev.* **D65** (2002) 083512, hep-th/0109024.
- [9] E. Abdalla and A. G. Casali, hep-th/0208008.
- [10] J.W. Moffat, hep-th/0208122.
- [11] C. Csáki, M.Graesser, L. Randall and J. Terning, *Phys. Rev.* **D62**, (2000) 045015, hep-th/9911406; P. Binetruy, C. Deffayet, D. Langlois *Nucl.Phys.* **B615**, (2001) 219, hep-th/0101234.
- [12] E. W. Kolb and M. S. Turner, *The Early Universe*, Addison-Wesley 1990.
- [13] G. Giudice, E. Kolb and J. Lesgourgues, hep-ph/0207145.
- [14] Shin'ichi Nojiri, Sergei D. Odintsov, Akio Sugamoto, *Mod. Phys. Lett.* **A17** (2002) 1269-1276; Shin'ichi Nojiri, Sergei D. Odintsov, *JHEP* **0112** (2001) 001, hep-th/0107134; Bin Wang, Elcio Abdalla, Ru-Keng Su, *Mod. Phys. Lett.* **A17** (2002) 23-30, hep-th/0106086.
- [15] Gibbons and S. Hawking *Phys. Rev.* **D 15** (1977) 2738-2751.
- [16] W. Israel, *Nuovo Cim.* **44B**, 1 (1966).
- [17] H.A.Chamblin and H.S.Reall, *Nucl.Phys.* **B** hep-th/9903225.
- [18] D. Ida, *JHEP* 0009 (2000) [gr-qc/9912002].
- [19] P. Kraus, *JHEP* 9912:011 (1999) hep-th/9910140.
- [20] P. Bowcock, C. Charmousis and R. Gregory, *Class. Quant. Grav.*, **17**, 4745 (2000), hep-th/0007177.
- [21] P. Binetruy, C. Deffayet and D. Langlois, *Nucl. Phys.* **B565**, (2000) 269, hep-th/9905012.
- [22] C. Csáki, M. Graesser, C. Kolda and J. Terning, *Phys. Lett.* **B462** 34 (1999), hep-ph/9906513.
- [23] J. Cline, C. Grosjean and G. Servant, *Phys. Rev. Lett.* **83** 4245 (1999), hep-ph/9906523.

- [24] P. Binetruy, C. Deffayet, U. Ellwanger and D. Langlois, *Phys. Lett.* **462B** 34 (1999) hep-th/9910219.
- [25] P. de Bernardis *et al.*, *Nature* **404**, 955 (2000); R. Stompor *et al.*, *Astrophys. J.* **561**, L7 (2001).